Available online at www.sciencedirect.com
ScienceDirect
Mathematics and Computers in Simulation 80 (2010) 1821–1840
MATHEMATICS AND COMPUTERS IN SIMULATION
www.elsevier.com/locate/matcom

A finite volume scheme for cardiac propagation in media with isotropic conductivities

Mostafa Bendahmane [a], Raimund Bürger [b], Ricardo Ruiz-Baier [c,*]

[a] *Institut de Mathématiques de Bordeaux, Université Victor Segalen – Bordeaux 2, 33076 Bordeaux, France*
[b] *CI²MA and Departamento de Ingeniería Matemática, Universidad de Concepción, Casilla 160-C, Concepción, Chile*
[c] *Modeling and Scientific Computing CMCS, École Polytechnique Fédérale de Lausanne EPFL, CH-1015 Lausanne, Switzerland*

Received 4 May 2009; received in revised form 8 September 2009; accepted 15 December 2009
Available online 4 January 2010

Abstract

A finite volume method for solving the monodomain and bidomain models for the electrical activity of myocardial tissue is presented. These models consist of a parabolic PDE and a system of a parabolic and an elliptic PDE, respectively, for certain electric potentials, coupled to an ODE for the gating variable. The existence and uniqueness of the approximate solution is proved, and it is also shown that the scheme converges to the corresponding weak solutions for the monodomain model, and for the bidomain model when considering diagonal conductivity tensors. Numerical examples in two and three space dimensions are provided, indicating experimental rates of convergence slightly above first order for both models.

MSC: 65M60; 65M12; 35K65; 35M10

Keywords: Axially symmetric bidomain model; Reaction–diffusion system; Finite volume approximation; Convergence to the weak solution

1. Introduction

1.1. Scope

The so-called bidomain model in electrocardiology (see e.g. [16,23,32]) is the most widely used model to describe the electrical activity (the propagation of action potential) in a slice of the cardiac muscle. In this model, the myocardium is regarded as a two-phase medium consisting in two interpenetrating and superimposed (anisotropic) continuous media, the intracellular (i) and extracellular (e) tissues, which occupy the same three-dimensional area and are separated from each other (and connected at each point) by the cardiac cellular membrane. It is the aim of the present paper to present a finite volume (FV) scheme for the numerical simulation of this model. The proposed scheme is supported by a convergence analysis and numerical examples illustrate its good behaviour. The scheme may be particularly useful as a building block for adaptive simulation tools in electrocardiology.

* Corresponding author. Tel.: +41 216932909; fax: +41 216934303.
E-mail addresses: mostafa_bendahmane@yahoo.fr (M. Bendahmane), rburger@ing-mat.udec.cl (R. Bürger), ricardo.ruiz@epfl.ch (R. Ruiz-Baier).

0378-4754/$36.00
doi:10.1016/j.matcom.2009.12.010

The underlying model is given by the following system, formed by a scalar parabolic PDE, coupled with an elliptic PDE and a time-dependent ODE:

$$\beta c_{\mathrm{m}} \partial_t v + \operatorname{div}(\mathbf{M}_{\mathrm{e}}(x)\nabla u_{\mathrm{e}}) + \beta I_{\mathrm{ion}}(v, w) = I_{\mathrm{app}}, \tag{1.1a}$$

$$\operatorname{div}((\mathbf{M}_{\mathrm{i}}(x) + \mathbf{M}_{\mathrm{e}}(x))\nabla u_{\mathrm{e}}) + \operatorname{div}(\mathbf{M}_{\mathrm{i}}(x)\nabla v) = I_{\mathrm{app}}, \tag{1.1b}$$

$$\partial_t w - H(v, w) = 0, \qquad (x, t) \in \Omega_T := \Omega \times (0, T], \tag{1.1c}$$

where $\Omega \subset \mathbb{R}^3$ is an open, bounded, connected polygonal domain with boundary $\partial\Omega$. The sought quantities are the intracellular and extracellular electric potentials $u_{\mathrm{i}} = u_{\mathrm{i}}(x, t)$ and $u_{\mathrm{e}} = u_{\mathrm{e}}(x, t)$. Their difference $v = v(x, t) = u_{\mathrm{i}} - u_{\mathrm{e}}$ is known as the transmembrane potential, and $w(x, t)$ is the so-called gating variable. The conductivity of the tissue is represented by scaled tensors $\mathbf{M}_{\mathrm{i}}(x)$ and $\mathbf{M}_{\mathrm{e}}(x)$ given in the axisymmetric or axially isotropic case by

$$\mathbf{M}_j(x) = \sigma_j^{\mathrm{t}}\mathbf{I} + (\sigma_j^{\mathrm{l}} - \sigma_j^{\mathrm{t}})\mathbf{a}_{\mathrm{l}}(x)\mathbf{a}_{\mathrm{l}}^{\mathrm{T}}(x),$$

where $\sigma_j^{\mathrm{l}} = \sigma_j^{\mathrm{l}}(x) \in C^1(\mathbb{R}^3)$ and $\sigma_j^{\mathrm{t}} = \sigma_j^{\mathrm{t}}(x) \in C^1(\mathbb{R}^3)$ for $j \in \{\mathrm{e},\mathrm{i}\}$ are the intra- and extracellular conductivities along and across the direction of the fiber. In the special case studied herein, $\mathbf{M}_{\mathrm{i}}(x)$ and $\mathbf{M}_{\mathrm{e}}(x)$ are assumed to be diagonal tensors. The term $\mathbf{M}_{\mathrm{i}}(x) + \mathbf{M}_{\mathrm{e}}(x)$ in (1.1b) is the tensor accounting for the bulk conductivity in the model. Moreover, $c_{\mathrm{m}} > 0$ is the surface capacitance of the membrane and β is the surface-to-volume ratio. The stimulation currents $I_{\mathrm{app}} = I_{\mathrm{app}}(x, t)$ applied to the intra- and extracellular space are assumed to satisfy the condition

$$\int_\Omega I_{\mathrm{app}}(x, t)\,\mathrm{d}x = 0 \quad \text{for a.e. } t \in (0, T).$$

In the special case where the conductivity tensors are assumed to be proportional, i.e. $\mathbf{M}_{\mathrm{i}} \equiv \mu\mathbf{M}_{\mathrm{e}}$ for some $\mu \in \mathbb{R}$, (1.1) is equivalent to a parabolic reaction-diffusion equation describing the evolution of the transmembrane potential v coupled with an ODE modelling the ionic and membrane currents. Such a simplified model is given by the following system, known as the monodomain model:

$$\begin{aligned} &\beta c_{\mathrm{m}} \partial_t v - \operatorname{div}\left(\frac{\mathbf{M}_{\mathrm{i}}}{1+\mu}\nabla v\right) + \beta I_{\mathrm{ion}}(v, w) = \frac{\mu}{1+\mu} I_{\mathrm{app}}, \\ &\partial_t w - H(v, w) = 0, \qquad (x, t) \in \Omega_T. \end{aligned} \tag{1.2}$$

This model is, of course, significantly less involved and requires substantially less computational effort than the bidomain model, and even though the assumption of equal anisotropy ratios is very strong and generally unrealistic, the monodomain model is still adequate for a qualitative investigation of certain repolarization sequences and the distribution of patterns of durations of the action potential, see e.g. [15].

1.2. Related work

The well-posedness of the bidomain model has been studied by several groups of authors. Just to mention a few results, Colli Franzone and Savaré [16] present a weak formulation for the bidomain model and show that it has a structure suitable to apply the theory of evolution variational inequalities in Hilbert spaces. Bendahmane and Karlsen [6] prove existence and uniqueness for the bidomain equations using the Faedo–Galerkin method and compactness theory for the existence proof. Veneroni [35] derives existence, uniqueness and regularity results for a slightly different version of the degenerate bidomain equations, and Bourgault, Coudière and Pierre [9] prove existence and uniqueness for the bidomain equations by first reformulating the problem into a single parabolic PDE and then applying a semigroup approach.

In recent years, the study of mathematical models for the propagation of electrical waves in the cardiac tissue has received many contributions in the framework of numerical methods and simulations. Among these studies, in the context of finite volume schemes, we mention the contribution of Harrild and Henriquez [22], who give one of the first approaches of FV methods for cardiac problems, and Trew et al. [34] introduce a FV scheme for the bidomain equations but representing physical discontinuities without the implicit removal of intracellular volume, which gives rise to linear instead of nonlinear systems. However, concerning the convergence of FV methods in the framework of electrophysiological problems, only a few works are available. Coudière and Pierre [18] give stability conditions for two time-stepping

methods in different settings, and they prove convergence of an implicit FV approximation to the monodomain equations. In a different spirit, a discrete duality FV method (DDFV) to solve the fully coupled heart and torso problem is presented by Coudière et al. [19], who prove well-posedness of the problem and present various numerical tests using preconditioning. Further contributions include the work by Bendahmane and Karlsen [7], who analyzed a FV method for another version of the bidomain equations, consisting in a system of two parabolic equations with Dirichlet boundary conditions. They proved existence, uniqueness and convergence of solutions to the FV scheme, and the present treatment is based on a similar approach, but we herein analyze a parabolic-elliptic system with Neumann boundary conditions, and we also provide numerical experiments. We also stress that the importance of our approach lies in the use of "standard", and therefore more easily handled, finite volume methods in the study of a special form of the bidomain equations.

Most of the recently developed simulation tools in electrocardiology do, however, not consist in a simple implementation of a reference scheme such as the FV scheme presented herein, but rather employ techniques of space- and time-adaptivity that take into account that the monodomain and bidomain models produce strongly localized solutions. For instance, the width of an excitation front is usually several orders of magnitude smaller than the long axis of a human-size right ventricle. From a computational point of view, substantial contributions have been made in adaptivity for cardiac models, which include adaptive mesh refinement (AMR) (e.g. [11]), adaptive finite element methods using a posteriori error techniques (see, e.g. [12]) and a domain decomposition approach using an alternating direction implicit (ADI) method (see Quan et al. [29]). Sundnes et al. [33] introduce an operator splitting method to solve a fully coupled discretization of three PDEs modelling the interaction between the myocardium and the torso surrounding the heart. Moreover, Skouibine et al. [31] present a predictor–corrector time stepping strategy to accelerate a given finite difference scheme for the bidomain equations using active membrane kinetics (the so-called BRDR model, named after the authors of [3,20]). Cherry et al. [11] use local time stepping, similar to the method by Berger and Oliger [8], to accelerate a reference scheme. Parallelized versions of part of these methods are presented, for example, by Colli Franzone and Pavarino [13] and Saleheen and Ng [30]. We conclude this short review of adaptive treatments mentioning that in [5] we advance an explicit version of the FV scheme presented herein augmented with a space–time adaptive multiresolution technique, which yields a fully adaptive, efficient numerical method for the anisotropic bidomain model, allowing also for more general conductivity tensors.

1.3. Outline of the paper

The remainder of this paper is organized as follows. In Section 2, after introducing the membrane model to be used, we define weak solutions to (1.1) and (1.2). Then we define the FV scheme used to approximate the bidomain model (1.1), which follows the framework of [21], and state our main results. In Section 3 it is shown by a fixed-point argument that the implicit FV formulation has unique solution, so that the FV scheme is indeed well-defined. Next, in Section 4, we first derive several discrete energy estimates for the our FV scheme, which are a required for the convergence proof; and then, after stating space and time translation estimates, we pass to the limit to conclude that the scheme converges to a weak solution of the bidomain model or of the monodomain model. In Section 5 we present two numerical examples, which simulate the propagation of action potential over simple geometries. These results put into evidence the good performance of the scheme, and we the corresponding error histories provided, show an experimental rate of convergence near $\mathcal{O}(h)$, where h is the meshsize. Finally, in Section 6 we present some conclusions and address the limitations of our treatment.

2. Preliminaries

In this section, we introduce the notations and basic results concerning the continuous model (1.1) that we will need in the next sections in order to construct and prove convergence of the corresponding numerical scheme. We also construct here the final form of the discrete equations, and state our main result.

2.1. Membrane models

The functions H and I_{ion} in (1.1) can be chosen according to the widely known FitzHugh-Nagumo model (see e.g. [23]), which for parameters $a, b, \theta \geq 0$ and $\lambda < 0$, is given by

$$H(v, w) = av - bw, \quad I_{\text{ion}}(v, w) = \lambda(v(1 - v)(v - \theta) - w). \tag{2.1}$$

An alternative is the Mitchell–Schaeffer membrane model [28]

$$H(v,w)=\frac{w_\infty(v/v_p)-w}{R_{\mathrm{m}}c_{\mathrm{m}}\eta_\infty(v/v_p)},\quad I_{\mathrm{ion}}(v,w)=\frac{v_p}{R_{\mathrm{m}}}\left(\frac{v}{v_p\eta_2}-\frac{v^2(1-v/v_p)w}{v_p^2\eta_1}\right), \tag{2.2}$$

where the dimensionless functions $\eta_\infty(s)$ and $w_\infty(s)$ are given by $\eta_\infty(s)=\eta_3+(\eta_4-\eta_3)\mathcal{H}(s-\eta_5)$ and $w_\infty(s)=\mathcal{H}(s-\eta_5)$, $\mathcal{H}$ is the Heaviside function, R_{m} is the surface resistivity of the membrane, and v_p and $\eta_1,\dots,\eta_5$ are given parameters.

Although numerical results shown in Section 5 indicate that the scheme converges for both membrane models (2.1) and (2.2), our well-definedness and convergence analysis is based on assumptions that are met by model (2.1) only. Specifically, for that model one can decompose I_{ion} as

$$I_{\mathrm{ion}}(v,w)=:I_{1,\mathrm{ion}}(v)+I_{2,\mathrm{ion}}(w).$$

Then it is straightforwardly seen that there exists a constant $C_I>0$ such that (see e.g. [16])

$$\frac{I_{1,\mathrm{ion}}(v_1)-I_{1,\mathrm{ion}}(v_2)}{v_1-v_2}\geq -C_I,\quad \forall v_1\neq v_2. \tag{2.3}$$

Additionally, there is a constant $C_I'>0$ such that

$$0<\liminf_{|v|\to\infty}\left|\frac{I_{1,\mathrm{ion}}(v)}{v^3}\right|\leq\limsup_{|v|\to\infty}\left|\frac{I_{1,\mathrm{ion}}(v)}{v^3}\right|\leq C_I'. \tag{2.4}$$

Inequalities (2.3) and (2.4) will be needed for the proofs of uniqueness of a weak solution and of the convergence of the numerical scheme, respectively.

2.2. Initial and boundary conditions

For sake of simplicity, we augment (1.1) with zero-flux boundary conditions, representing an isolated piece of cardiac tissue:

$$(\mathbf{M}_j(x)\nabla u_j)\cdot\mathbf{n}=0\quad\text{on}\quad \Sigma_T:=\partial\Omega\times(0,T),\quad j\in\{\mathrm{e},\mathrm{i}\}. \tag{2.5}$$

Furthermore, the transmembrane potential and the gating variable are assumed to be known. Therefore we have the initial conditions (which are degenerate for the potentials u_{i}, u_{e}):

$$v(x,0)=v_0(x),\quad w(x,0)=w_0(x),\quad x\in\Omega. \tag{2.6}$$

If we fixed both $u_{\mathrm{e}}(x,0)$ and $u_{\mathrm{i}}(x,0)$ as independent initial data, the problem could become unsolvable, since the time derivative involves only $v=u_{\mathrm{i}}-u_{\mathrm{e}}$ (this is also referred to as d egeneracy in time). Moreover, u_{i} and u_{e} (as all electrical potentials defined on bounded domains) are defined up to an additive constant, while v is uniquely determined. In our case, this constant is usually chosen so that the following condition holds (see e.g. [15])

$$\int_\Omega u_{\mathrm{e}}(x,t)\,\mathrm{d}x=0\quad\text{for a.e. } t\in(0,T). \tag{2.7}$$

2.3. Weak solutions

We assume that $I_{\mathrm{app}}\in L^2(\Omega_T)$ and that there exists a constant $C_M>0$ such that

$$\mathbf{M}_j\in L^\infty(\Omega),\quad \mathbf{M}_j\xi\cdot\xi\geq C_M|\xi|^2\quad\text{for a.e. } x\in\Omega,\quad\text{for all }\xi\in\mathbb{R}^3,\ j\in\{\mathrm{e},\mathrm{i}\}. \tag{2.8}$$

Definition 2.1. A weak solution of (1.1), (2.5) and (2.6) is a triple $\mathbf{u} = (v, u_e, w)$ of functions such that $v, u_e \in L^2(0, T; H^1(\Omega))$, $w \in C([0, T], L^2(\Omega))$, (2.7) is satisfied, and for all test functions $\varphi, \psi, \xi \in \mathcal{D}([0, T) \times \bar{\Omega})$,

$$\begin{aligned}
&-\beta c_m \int_\Omega v_0(x)\varphi(0,x)\,dx + \iint_{\Omega_T} (-\beta c_m v\partial_t\varphi - \mathbf{M}_e(x)\nabla u_e\cdot\nabla\varphi + \beta I_{ion}\varphi)\,dx\,dt = \iint_{\Omega_T} I_{app}\varphi\,dx\,dt,\\
&\iint_{\Omega_T} (\mathbf{M}_i(x)+\mathbf{M}_e(x))\nabla u_e\cdot\nabla\psi\,dx\,dt = -\iint_{\Omega_T} \mathbf{M}_i(x)\nabla v\cdot\nabla\psi\,dx\,dt - \iint_{\Omega_T} I_{app}\varphi\,dx\,dt,\\
&-\int_\Omega w_0(x)\xi(0,x)\,dx - \iint_{\Omega_T} w\partial_t\xi\,dx\,dt = \iint_{\Omega_T} H\xi\,dx\,dt.
\end{aligned} \tag{2.9}$$

Definition 2.2. A pair $\mathbf{u} = (v, w)$ is a weak solution of the monodomain model (1.2) if $v \in L^2(0, T; H^1(\Omega))$, $w \in C([0, T], L^2(\Omega))$, and the following identities hold for all test functions $\varphi, \xi \in \mathcal{D}([0, T) \times \bar{\Omega})$:

$$\begin{aligned}
&-\beta c_m \int_\Omega v_0(x)\varphi(0,x)\,dx + \iint_{\Omega_T} \left\{-\beta c_m v\partial_t\varphi + \beta I_{ion}\varphi + \frac{1}{1+\mu}\mathbf{M}_i\nabla v\cdot\nabla\varphi\right\} dx\,dt = \frac{\mu}{1+\mu}\iint_{\Omega_T} I_{app}\varphi\,dx\,dt,\\
&-\int_\Omega w_0(x)\xi(0,x)\,dx - \iint_{\Omega_T} w\partial_t\xi\,dx\,dt = \iint_{\Omega_T} H\xi\,dx\,dt.
\end{aligned}$$

2.4. The finite volume scheme

2.4.1. Admissible mesh

We employ for our discretization a mesh formed by a family $\mathcal{T}$ of control volumes, which are restricted to be open rectangles of maximum diameter h. We refer to the parameter h as mesh size. Of course, the mesh should be *admissible* in the sense of [21].

For all $K \in \mathcal{T}$, x_K denotes the center of K, $\mathcal{E}(K)$ is the set of edges of K, $\mathcal{E}_{int}(K)$ corresponds to those is in the interior of $\mathcal{T}$ and $\mathcal{E}_{ext}(K)$ is the set of edges of K lying on the boundary $\partial\Omega$, i.e.

$$\mathcal{E}(K) = \mathcal{E}_{int}(K) \cup \mathcal{E}_{ext}(K), \quad \mathcal{E}_{int}(K) \cap \mathcal{E}_{ext}(K) = \emptyset \quad \text{for all } K \in \mathcal{T}.$$

By $\mathcal{E}_{int}$ and $\mathcal{E}_{ext}$ we will denote the sets of all edges in the interior of $\mathcal{T}$ and lying on the boundary $\partial\Omega$, respectively. For a given finite volume K, we denote by $N(K)$ the set of neighbors of K which share a common edge with K. For all $L \in N(K)$, $d(K, L)$ denotes the distance between x_K and x_L and $\sigma = K|L$ (respectively $\sigma = K|\partial\Omega$) is the interface between K and L (between K and the boundary $\partial\Omega$, respectively). Moreover, $\eta_{K,\sigma}$ is the unit normal vector to $\sigma = K|L$ ($\sigma \in \mathcal{E}_{ext}(K)$, respectively) oriented from K to L (from K to $\partial\Omega$, respectively). For all $K \in \mathcal{T}$, $|K|$ stands for the measure of the cell K. We have that $\bar{\Omega} = \cup_{K\in\mathcal{T}}\bar{K}$, $K \cap L = \varnothing$ if $K, L \in \mathcal{T}$ and $K \neq L$, and the orthogonality property between $\overline{x_K x_L}$ and $\sigma = K|L$ is satisfied in particular by rectangular control volumes. The admissible mesh satisfies in particular the following regularity condition: for some $\alpha \in \mathbb{R}^+$

$$\min_{K\in\mathcal{T}, L\in N(K)} \frac{d(K,L)}{\mathrm{diam}(K)} \geq \alpha.$$

Clearly, the concept of admissibility introduced in [21] is defined for more general meshes. However, for ease of reference we will refer herein to a rectangular mesh satisfying the conditions stated herein as an *admissible rectangular mesh*.

2.4.2. Approximation of the bidomain model

To discretize (1.1), we choose an admissible discretization of Ω_T, consisting of an admissible mesh of Ω and a time step size $\Delta t > 0$. We may choose $N > 0$ as the smallest integer such that $N\Delta t \geq T$, and set $t^n := n\Delta t$ for $n \in \{0, \ldots, N\}$. On each cell $K \in \mathcal{T}$, let us define positive definite conductivity tensors by

$$\mathbf{M}_{j,K} := \frac{1}{|K|}\int_K \mathbf{M}_j(x)\,dx, \quad j \in \{e, i\}. \tag{2.10}$$

Utilizing the quantities (2.10), we can now define the following approximation of the mean flux along $\sigma \in \mathcal{E}(K)$ of a variable $q \in \{u_e, v\}$ across that edge, which also incorporates the zero-flux boundary condition for external edges

$\sigma \in \mathcal{E}_{\rm ext}(K)$:

$$F_{j,q,K,\sigma} \begin{cases} \approx \displaystyle\int_\sigma (\mathbf{M}_j(x)\nabla q)\cdot \eta_{K,\sigma}\,\mathrm{d}\gamma & \text{for } \sigma \in \mathcal{E}_{\rm int}(K),\ j \in \{\mathrm{e},\mathrm{i}\},\ q \in \{u_\mathrm{e}, v\}, \\ = 0 & \text{for } \sigma \in \mathcal{E}_{\rm ext}(K),\ j \in \{\mathrm{e},\mathrm{i}\},\ q \in \{u_\mathrm{e}, v\}. \end{cases}$$

For internal edges, i.e. $\sigma \in \mathcal{E}_{\rm int}(K)$, let us define

$$M_{j,K,\sigma} = |\mathbf{M}_{j,K}\eta_{K,\sigma}|, \quad j \in \{\mathrm{e},\mathrm{i}\}.$$

The diffusive fluxes

$$\mathbf{M}_j(x)\nabla q \cdot \eta_{K,\sigma} \quad \text{on } \sigma = K|L \in \mathcal{E}_{\rm int}(K), \quad q \in \{u_\mathrm{e}, v\}$$

are approximated by

$$\frac{1}{|\sigma|}\int_\sigma (\mathbf{M}_j(x)\nabla q)\cdot \eta_{K,\sigma}\,\mathrm{d}\gamma \approx \nabla q(y_\sigma)\cdot(\mathbf{M}_{j,K}\,\eta_{K,\sigma}) = M_{j,K,\sigma}\nabla q(y_\sigma)\cdot\frac{y_\sigma - x_K}{d(K,\sigma)} \approx M_{j,K,\sigma}\frac{q_\sigma - q_K}{d(K,\sigma)}, \tag{2.11}$$

where y_σ is the center of σ and q_σ is an approximation of $q(y_\sigma)$, $q \in \{u_\mathrm{e}, v\}$. Obviously, the latter represent auxiliary unknowns. By imposing conservativity of the scheme, it is possible to determine the additional unknowns $q_\sigma, q \in \{u_\mathrm{e}, v\}$, and to compute the numerical fluxes on all edges as follows:

$$F_{j,q,K,\sigma} = \begin{cases} d^*_{j,\sigma}(q_L - q_K) & \text{for } \sigma = K|L \in \mathcal{E}_{\rm int}(K),\ j \in \{\mathrm{e},\mathrm{i}\},\ q \in \{u_\mathrm{e}, v\}, \\ 0 & \text{for } \sigma \in \mathcal{E}_{\rm ext}(K),\ j \in \{\mathrm{e},\mathrm{i}\},\ q \in \{u_\mathrm{e}, v\}, \end{cases} \tag{2.12}$$

where we define

$$d^*_{j,\sigma} := \frac{M_{j,K,\sigma}M_{j,L,\sigma}|\sigma|d(K,L)}{d(K,\sigma)M_{j,K,\sigma} + d(L,\sigma)M_{j,L,\sigma}} \quad \text{for } \sigma = K|L \in \mathcal{E}_{\rm int}(K). \tag{2.13}$$

When $\mathbf{M}_\mathrm{i}$ and $\mathbf{M}_\mathrm{e}$ are diagonal tensors, the resulting approximation of fluxes is consistent (see [21]). However, the above flux computation is not consistent in the general anisotropic case; more precisely, the equality in (2.11) does not hold in that case. For a brief discussion, see Remark 2.1 at the end of this section.

We denote the cell averages of u_e, v and w on $K \in \mathcal{T}$ at time $t = t^n$ by the respective expressions

$$u^n_{\mathrm{e},K} := \frac{1}{|K|}\int_K u_\mathrm{e}(x,t^n)\,\mathrm{d}x, \quad v^n_K := \frac{1}{|K|}\int_K v(x,t^n)\,\mathrm{d}x, \quad w^n_K := \frac{1}{|K|}\int_K w(x,t^n)\,\mathrm{d}x,$$

and let $F^n_{j,q,K,\sigma}$ denote the quantities obtained from replacing q_K and q_L in (2.12) by q^n_K and q^n_L, i.e.

$$F^n_{j,q,K,\sigma} = \begin{cases} d^*_{j,\sigma}(q^n_L - q^n_K) & \text{for } \sigma = K|L \in \mathcal{E}_{\rm int}(K),\ j \in \{\mathrm{e},\mathrm{i}\},\ q \in \{u_\mathrm{e}, v\}, \\ 0 & \text{for } \sigma \in \mathcal{E}_{\rm ext}(K),\ j \in \{\mathrm{e},\mathrm{i}\},\ q \in \{u_\mathrm{e}, v\}, \end{cases} \tag{2.14}$$

where $d^*_{j,\sigma}$ is defined in (2.13). Furthermore, we define the unknowns

$$H^n_K := H(v^n_K, w^n_K), \quad I^n_{\mathrm{ion},K} := I_{\rm ion}(v^n_K, w^n_K),$$

and the cell averages of the given function $I_{\rm app}$ at time $t = t^n$:

$$I^n_{\mathrm{app},K} := \frac{1}{|K|}\int_K I_{\rm app}(x,t^n)\,\mathrm{d}x.$$

The computation starts from the initial cell averages

$$v^0_K = \frac{1}{|K|}\int_K v_0(x)\,\mathrm{d}x, \quad w^0_K = \frac{1}{|K|}\int_K w_0(x)\,\mathrm{d}x. \tag{2.15}$$

2.4.3. Time stepping

To advance the numerical solution from t^n to $t^{n+1} = t^n + \Delta t$, we use the following FV scheme: given $u^n_{e,K}$, v^n_K and w^n_K for all $K \in \mathcal{T}$ at time $t = t^n$, determine $u^{n+1}_{e,K}$, v^{n+1}_K and w^{n+1}_K for all $K \in \mathcal{T}$ at time $t = t^{n+1} = t^n + \Delta t$ from the following discrete versions of (1.1a)–(1.1c):

$$\beta c_m |K| \frac{v^{n+1}_K - v^n_K}{\Delta t} + \sum_{\sigma \in \mathcal{E}(K)} F^{n+1}_{e,u_e,K,\sigma} + \beta |K| I^{n+1}_{ion,K} = |K| I^{n+1}_{app,K}, \tag{2.16}$$

$$\sum_{\sigma \in \mathcal{E}(K)} (F^{n+1}_{i,u_e,K,\sigma} + F^{n+1}_{e,u_e,K,\sigma} + F^{n+1}_{i,v,K,\sigma}) = |K| I^{n+1}_{app,K}, \tag{2.17}$$

$$\frac{w^{n+1}_K - w^n_K}{\Delta t} - H^{n+1}_K = 0. \tag{2.18}$$

Note that due to our definition (2.14) this scheme appropriately incorporates the zero-flux boundary conditions.

2.4.4. Final form of the FV scheme

For the subsequent analysis we find it more convenient to rewrite the scheme in the following equivalent way, where zero summands (due to the zero-flux boundary condition) that occur in (2.16) and (2.17) are avoided by summing for each $K \in \mathcal{T}$ over $\sigma \in \mathcal{E}_{int}(K)$ rather than $\sigma \in \mathcal{E}(K)$. Thus, final form of the scheme incorporates the boundary condition (2.5). Moreover, we denote by $\tilde{u}^{n+1}_{e,K}$ is a preliminary version of $u^{n+1}_{e,K}$ for $K \in \mathcal{T}$. After each time step, these values are normalized to ensure that a discrete version of the compatibility condition (2.7) holds. The final form of the scheme is as follows:

$$\beta c_m |K| \frac{v^{n+1}_K - v^n_K}{\Delta t} + \sum_{\sigma \in \mathcal{E}_{int}(K)} d^*_{e,\sigma} (\tilde{u}^{n+1}_{e,L} - \tilde{u}^{n+1}_{e,K}) + \beta |K| I^{n+1}_{ion,K} = |K| I^{n+1}_{app,K}, \tag{2.19}$$

$$\sum_{\sigma \in \mathcal{E}_{int}(K)} \{(d^*_{i,\sigma} + d^*_{e,\sigma})(\tilde{u}^{n+1}_{e,L} - \tilde{u}^{n+1}_{e,K}) + d^*_{i,\sigma}(v^{n+1}_L - v^{n+1}_K)\} = |K| I^{n+1}_{app,K}, \tag{2.20}$$

$$\frac{w^{n+1}_K - w^n_K}{\Delta t} - H^{n+1}_K = 0 \tag{2.21}$$

for all $K \in \mathcal{T}$, and condition (2.7) is imposed via the normalization

$$u^{n+1}_{e,K} = \tilde{u}^{n+1}_{e,K} - \sum_{L \in \mathcal{T}} |K| \tilde{u}^{n+1}_{e,L} \quad \text{for all } K \in \mathcal{T}, \quad n \in \{0, \ldots, N-1\}. \tag{2.22}$$

In order to prove existence and uniqueness of a solution to (2.15), (2.19)–(2.22) we will assume that the following mild time step condition is satisfied:

$$\Delta t < \frac{\beta c_m}{2\beta C_I + (\beta^2 \lambda^2 / b) + (a^2/b)}, \tag{2.23}$$

where a, b, λ are the parameters of the FitzHugh-Nagumo model (2.1). For simplicity of notation we introduce

$$u_{e,h}(x,t) = u^{n+1}_{e,K}, \quad w_h(x,t) = w^{n+1}_K, \quad v_h(x,t) = v^{n+1}_K \quad \text{for all } (x,t) \in (n\Delta t, (n+1)\Delta t] \times K,$$

with $K \in \mathcal{T}$ and $n \in \{0, \ldots, N-1\}$; and we define $\mathbf{u} := (u_e, v, w)$ and $\mathbf{u}_h := (u_{e,h}, v_h, w_h)$.

2.5. Statement of the main result and further remarks

The convergence of the FV method given above is established by our main result, formulated as follows.

Theorem 2.1. *Suppose that $v_0 \in L^2(\Omega)$, $w_0 \in L^2(\Omega)$ and $I_{ion} \in L^2(Q_T)$, $I_{app} \in L^2(Q_T)$. Then the FV solution $\mathbf{u}_h$, generated by (2.15), (2.19)–(2.22), converges along a subsequence to $\mathbf{u}$ as $h \to 0$, where $\mathbf{u}$ i s a weak solution of (1.1),*

(2.5), (2.6). *The convergence is understood in the following sense*:

$$v_h \to v \text{ strongly in } L^2(Q_T) \text{ and a.e. in } Q_T,$$
$$\nabla_h u_{e,h} \to \nabla u_e \text{ weakly in } (L^2(Q_T))^3,$$
$$w_h \to w \text{ weakly in } L^2(Q_T).$$

Remark 2.1. Note that our FV scheme is only consistent in the case where the diffusion matrices are both isotropic, as for example in the monodomain model. Specifically, we stress that the first equality in (2.11) is not true in general but only if $\mathbf{M}_{j,K}\eta_{K,\sigma} = |\mathbf{M}_{j,K}\eta_{K,\sigma}|\eta_{K,\sigma}$, which is only the case if $\eta_{K,\sigma}$ is an eigenvector of $M_{j,K}$. Furthermore, the underlying scheme cannot be modified in a simple manner to be consistent in general for the bidomain equations. To overcome this difficulty, several variants of the proposed FV method have been recently proposed, such as the diamond scheme or the DDFV method (see e.g. [1,19]).

Remark 2.2. We also emphasize that since the proof of Theorem 2.1 is based on a compactness argument, we do not provide theoretical error estimates. Nevertheless, the numerical results given in Section 5 yield information about the experimental rate of convergence of the method.

Remark 2.3. As in [5], it is possible, at least formally, to deduce that an explicit version of the FV method (2.15)–(2.21) in the case of Cartesian meshes, is stable under the CFL condition

$$\Delta t \le h[2\max_{K\in\mathcal{T}}(|I_{\text{ion},K}| + 2|I_{\text{app},K}|) + 4h^{-1}\max_{K\in\mathcal{T}}(|\mathbf{M}_{\text{i},K}| + |\mathbf{M}_{\text{e},K}|)]^{-1}.$$

3. Well-definedness of the scheme

This section is devoted to the proof of existence and uniqueness of a solution to the FV method (2.19)–(2.21). Let $H_h(\Omega) \subset L^2(\Omega)$ be the space of piecewise constant functions on each $K \in \mathcal{T}$. For all $y_h \in H_h(\Omega)$ and for all $K \in \mathcal{T}$, y_K denotes the constant value of y_h in K. For $(y_h, z_h) \in (H_h(\Omega))^2$, we define

$$\langle y_h, z_h\rangle_{H_h} := \sum_{\sigma=K|L\in\mathcal{E}_{\text{int}}} d_\sigma^*(y_L - y_K)(z_L - z_K), \quad \|y_h\|_{H_h(\Omega)} := (\langle y_h, y_h\rangle_{H_h})^{1/2}.$$

We also define $L_h(\Omega) \subset L^2(\Omega)$ as the space of piecewise constant functions on each $K \in \mathcal{T}$ with the norm

$$(y_h, z_h)_{L_h(\Omega)} = \sum_{K\in\mathcal{T}} |K| y_K z_K, \qquad \|y_h\|^2_{L_h(\Omega)} = \sum_{K\in\mathcal{T}} |K||y_K|^2,$$

for $y_h, z_h \in L_h(\Omega)$. In the sequel we will drop the time step superscript whenever it is not needed.

To prove existence of solution to the discrete problem, we will need the following discrete Sobolev inequality (see e.g. [17]).

Lemma 3.1. *Let z be a function such that $|\Omega|^{-1}\int_\Omega z(x)\,dx = 0$ and z is constant on each cell of $\mathcal{T}$, that is, $z(x) = z_K$ if $x \in K$, $K \in \mathcal{T}$. Then there exists $C_p > 0$, depending on Ω, such that*

$$\|z\|^2_{L^2(\Omega)} \le C_p \|z\|^2_{H_h(\Omega)}. \tag{3.1}$$

Proposition 3.2. *Let $\mathcal{D}$ be an admissible rectangular discretization of Ω_T. Then the FV scheme (2.19)–(2.21) admits a unique solution $(u^n_{e,K}, u^n_{i,K}, w^n_K)$ with $u^n_{i,K} = v^n_K + u^n_{e,K}$ for all $K \in \mathcal{T}$ and $n \in \{1, \dots, N\}$.*

Notice that for technical purposes, here we equivalently establish the existence of the discrete solution $(u^n_{\text{e},K}, u^n_{\text{i},K}, w^n_K)$ instead of $(u^n_{\text{e},K}, v^n_K, w^n_K)$ for all $K \in \mathcal{T}$ and $n \in \{1, \dots, N\}$. For the proof we will appeal to the following classical lemma (see e.g. [24]).

Lemma 3.3. *Let $(\mathcal{A}, [\cdot,\cdot], \|\cdot\|)$ be a finite-dimensional Hilbert space, and let $\mathcal{P}$ be a continuous mapping from $\mathcal{A}$ into itself such that*

$$[\mathcal{P}(\xi), \xi] > 0 \quad \text{for all } \xi, \text{ with } \|\xi\| = r > 0.$$

Then there exists $\xi \in \mathcal{A}$ such that $\mathcal{P}(\xi) = 0$.

Proof of Proposition 3.2. Let $E_h := H_h(\Omega) \times H_h(\Omega) \times L_h(\Omega)$ be a Hilbert space endowed with the obvious norm, let $\Phi_h = (\psi_h, \varphi_h, \xi_h) \in E_h$ and define the bilinear forms A_h and B_h and the operator $\mathbf{C}^n$ via

$$\begin{aligned}
&A_h(\mathbf{u}_h^n, \Phi_h) := (\beta c_{\mathrm{m}} v_h^n, -\psi_h)_{L_h(\Omega)} + (w_h^n, \xi_h)_{L_h(\Omega)},\\
&B_h(\mathbf{u}_h^{n+1}, \Phi_h) := \sum_{K\in\mathcal{T}} \sum_{\sigma\in\mathcal{E}_{\mathrm{int}}(K)} (d^*_{\mathrm{e},\sigma}(u_{\mathrm{e},L}^{n+1} - u_{\mathrm{e},K}^{n+1})(\psi_L - \psi_K)\\
&\qquad + [(d^*_{\mathrm{i},\sigma} + d^*_{\mathrm{e},\sigma})(u_{\mathrm{e},L}^{n+1} - u_{\mathrm{e},K}^{n+1}) + d^*_{\mathrm{i},\sigma}(v_L^{n+1} - v_K^{n+1})](\varphi_L - \varphi_K)),\\
&(\mathbf{C}^{n+1}, \Phi_h)_h := \sum_{K\in\mathcal{T}} |K|(-\beta I_{\mathrm{ion},K}^{n+1}\psi_K + I_{\mathrm{app},K}^{n+1}\psi_K + I_{\mathrm{app},K}^{n+1}\varphi_K - H_K^{n+1}\xi_K),
\end{aligned}$$

where $\mathbf{u}_h = (u_{\mathrm{e},h}, u_{\mathrm{i},h}, w_h)$ with $u_{\mathrm{i},h} = v_h + u_{\mathrm{i},h}$. Multiplying (2.19) by ψ_K, (2.20) by φ_K, (2.21) by ξ_K, and summing the resulting equations for all $K \in \mathcal{T}$, we obtain

$$\frac{1}{\Delta t}(A_h(\mathbf{u}_h^{n+1}, \Phi_h) - A_h(\mathbf{u}_h^n, \Phi_h)) + B_h(\mathbf{u}_h^{n+1}, \Phi_h) + (\mathbf{C}^{n+1}, \Phi_h)_h = 0.$$

We now define the mapping $\mathcal{P} : E_h \to E_h$ by

$$[\mathcal{P}(\mathbf{u}_h^{n+1}), \Phi_h] = \frac{1}{\Delta t}(A_h(\mathbf{u}_h^{n+1}, \Phi_h) - A_h(\mathbf{u}_h^n, \Phi_h)) + B_h(\mathbf{u}_h^{n+1}, \Phi_h) + (\mathbf{C}^{n+1}, \Phi_h)_h \quad \text{for all } \Phi_h \in E_h$$

and apply Lemma 3.3 to obtain the existence of $\mathbf{u}_K^n = (u_{\mathrm{e},K}^n, u_{\mathrm{i},K}^n, w_K^n)$ for all $K \in \mathcal{T}, n \in \{0, \dots, N\}$. Using the discrete Hölder inequality, we deduce the continuity of A_h and B_h. Also, a standard verification leads to the continuity of the discrete form $(\mathbf{C}^{n+1}, \cdot)_h$. We then conclude that $\mathcal{P}$ is continuous and the task is now to show that

$$[\mathcal{P}(\mathbf{u}_h^{n+1}), \mathbf{u}_h^{n+1}] > 0 \quad \text{for } \|\mathbf{u}_h^{n+1}\|_{E_h} = r > 0$$

for a sufficiently large r. To this end, firstly observe that

$$\begin{aligned}
[\mathcal{P}(\mathbf{u}_h^{n+1}), \mathbf{u}_h^{n+1}] &= \sum_{K\in\mathcal{T}} |K| \left\{ -\frac{\beta c_{\mathrm{m}}}{\Delta t}(v_K^{n+1} - v_K^n)u_{\mathrm{e},L}^{n+1} + \frac{(w_K^{n+1})^2}{\Delta t} + \frac{1}{|K|}\sum_{\sigma\in\mathcal{E}_{\mathrm{int}}(K)} (d^*_{\mathrm{e},\sigma}(u_{\mathrm{e},L}^{n+1} - u_{\mathrm{e},K}^{n+1})^2 \right.\\
&\quad + [(d^*_{\mathrm{i},\sigma} + d^*_{\mathrm{e},\sigma})(u_{\mathrm{e},L}^{n+1} - u_{\mathrm{e},K}^{n+1}) + d^*_{\mathrm{i},\sigma}(v_L^{n+1} - v_K^{n+1})][v_L^{n+1} + u_{\mathrm{e},L}^{n+1} - (v_K^{n+1} + u_{\mathrm{e},K}^{n+1})])\\
&\quad \left. - \frac{w_K^n w_K^{n+1}}{\Delta t} - \beta I_{\mathrm{ion},K}^{n+1}u_{\mathrm{e},K}^{n+1} + 2I_{\mathrm{app},K}^{n+1}u_{\mathrm{e},K}^{n+1} + I_{\mathrm{app},K}^{n+1}v_K^{n+1} - H_K^{n+1}w_K^{n+1} \right\}\\
&= \sum_{K\in\mathcal{T}} |K| \left\{ -\frac{\beta c_{\mathrm{m}}}{\Delta t}(v_K^{n+1} - v_K^n)u_{\mathrm{e},L}^{n+1} + \frac{(w_K^{n+1})^2 - w_K^n w_K^{n+1}}{\Delta t} - \beta I_{\mathrm{ion},K}^{n+1}u_{\mathrm{e},K}^{n+1} \right.\\
&\quad + \frac{1}{|K|}\sum_{\sigma\in\mathcal{E}_{\mathrm{int}}(K)} (d^*_{\mathrm{e},\sigma}(u_{\mathrm{e},L}^{n+1} - u_{\mathrm{e},K}^{n+1})^2 + d^*_{\mathrm{i},\sigma}[v_L^{n+1} + u_{\mathrm{e},L}^{n+1} - (v_K^{n+1} + u_{\mathrm{e},K}^{n+1})]^2\\
&\quad + d^*_{\mathrm{e},\sigma}(u_{\mathrm{e},L}^{n+1} - u_{\mathrm{e},K}^{n+1})[v_L^{n+1} + u_{\mathrm{e},L}^{n+1} - (v_K^{n+1} + u_{\mathrm{e},K}^{n+1})]) + 2I_{\mathrm{app},K}^{n+1}u_{\mathrm{e},K}^{n+1}\\
&\quad \left. + I_{\mathrm{app},K}^{n+1}v_K^{n+1} - H_K^{n+1}w_K^{n+1} \right\}. \qquad (3.2)
\end{aligned}$$

Multiplying (2.19) by $(v_K^{n+1} + u_{e,K}^{n+1})$ and summing over all $K \in \mathcal{T}$ we arrive at

$$\sum_{K\in\mathcal{T}} |K| \left\{ \frac{\beta c_m}{\Delta t}(v_K^{n+1} - v_K^n)(v_K^{n+1} + u_{e,K}^{n+1}) + \beta I_{ion,K}^{n+1}(v_K^{n+1} + u_{e,K}^{n+1}) - I_{app,K}^{n+1}(v_K^{n+1} + u_{e,K}^{n+1}) \right\}$$
$$= \sum_{K\in\mathcal{T}} \sum_{\sigma\in\mathcal{E}_{int}(K)} d_{e,\sigma}^*(u_{e,L}^{n+1} - u_{e,K}^{n+1})[v_L^{n+1} + u_{e,L}^{n+1} - (v_K^{n+1} + u_{e,K}^{n+1})]. \tag{3.3}$$

Next, exploiting (3.3) we deduce from (3.2) that

$$[\mathcal{P}(\mathbf{u}_h^{n+1}), \mathbf{u}_h^{n+1}] = \sum_{K\in\mathcal{T}} |K| \left\{ \frac{\beta c_m}{\Delta t}(v_K^{n+1})^2 + \frac{(w_K^{n+1})^2}{\Delta t} - \frac{\beta c_m}{\Delta t} v_K^n v_K^{n+1} - \frac{w_K^n w_K^{n+1}}{\Delta t} + I_{app,K}^{n+1} u_{e,K}^{n+1} - H_K^{n+1} w_K^{n+1} \right.$$
$$\left. + \beta I_{ion,K}^{n+1} v_K^{n+1} + \frac{1}{|K|} \sum_{\sigma\in\mathcal{E}_{int}(K)} (d_{e,\sigma}^*(u_{e,L}^{n+1} - u_{e,K}^{n+1})^2 + d_{i,\sigma}^*[v_L^{n+1} + u_{e,L}^{n+1} - (v_K^{n+1} + u_{e,K}^{n+1})]^2) \right\}.$$

Given (2.8), writing explicitly H and I_{ion} as in (2.1), using Young's inequality, and from (3.1) it follows that

$$[\mathcal{P}(\mathbf{u}_h^{n+1}), \mathbf{u}_h^{n+1}] \geq \sum_{K\in\mathcal{T}} |K| \left\{ \frac{\beta c_m}{\Delta t}(v_K^{n+1})^2 + \frac{(w_K^{n+1})^2}{\Delta t} - \beta C_I (v_K^{n+1})^2 - \frac{b}{2}(w_K^{n+1})^2 - \frac{\beta^2\lambda^2}{2b}(v_K^{n+1})^2 \right.$$
$$+ b(w_K^{n+1})^2 - \frac{a^2}{2b}(v_K^{n+1})^2 - \frac{b}{2}(w_K^{n+1})^2 - C(C_M, C_p)(I_{app,K}^{n+1})^2 - \frac{C_M}{2C_p^2}(u_{e,h}^{n+1})^2$$
$$\left. - \frac{\beta c_m}{2\Delta t}(v_K^{n+1})^2 - \frac{(w_K^{n+1})^2}{2\Delta t} - C(c_m, \beta, \Delta t)(v_K^n)^2 - C(\Delta t)(w_K^n)^2 \right\}$$
$$+ C_M(\|v_h^{n+1} + u_{e,h}^{n+1}\|_{H_h(\Omega)}^2 + \|u_{e,h}^{n+1}\|_{H_h(\Omega)}^2),$$

and therefore we get

$$[\mathcal{P}(\mathbf{u}_h^{n+1}), \mathbf{u}_h^{n+1}] \geq \sum_{K\in\mathcal{T}} |K| \left\{ \left(\frac{\beta c_m}{2\Delta t} - \beta C_I - \frac{\beta^2\lambda^2}{2b} - \frac{a^2}{2b} \right) |v_K^{n+1}|^2 + \frac{|w_K^{n+1}|^2}{2\Delta t} \right.$$
$$\left. - C(C_M, C_p)|I_{app,K}^{n+1}|^2 - C(c_m, \beta, \Delta t)(v_K^n)^2 - C(\Delta t)(w_K^n)^2 \right\}$$
$$+ \frac{C_M}{2}(\|v_h^{n+1} + u_{e,h}^{n+1}\|_{H_h(\Omega)}^2 + \|u_{e,h}^{n+1}\|_{H_h(\Omega)}^2).$$

Finally, if we use (2.23), then, for a given $\mathbf{u}_h^n$ we can choose $\mathbf{u}_h^{n+1}$ with a sufficiently large norm to conclude the proof of existence of at least one solution to (2.19)–(2.21).

To prove uniqueness of this solution, let us first assume that there exists $n \in \{0, \ldots, N\}$ such that $u_{e,K}^n = \tilde{u}_{e,K}^n$, $v_K^n = \tilde{v}_K^n$ and $w_K^n = \tilde{w}_K^n$ for all $K \in \mathcal{T}$, but $u_{e,K}^{n+1} \neq \tilde{u}_{e,K}^{n+1}$, $v_K^{n+1} \neq \tilde{v}_K^{n+1}$ or $w_K^{n+1} \neq \tilde{w}_K^{n+1}$ for some $K \in \mathcal{T}$, all of these functions satisfying (2.19)–(2.21). In particular, and without loss of generality, let us assume that $v_L^{n+1} \neq \tilde{v}_L^{n+1}$ for some $L \in \mathcal{T}$(for the assumptions $u_{e,L}^{n+1} \neq \tilde{u}_{e,L}^{n+1}$ or $w_L^{n+1} \neq \tilde{w}_L^{n+1}$ for some $L \in \mathcal{T}$, one may proceed analogously). Substracting the scheme for $\{u_{e,K}^n, v_K^n, w_K^n\}$ from the scheme for $\{\tilde{u}_{e,K}^n, \tilde{v}_K^n, \tilde{w}_K^n\}$ and defining

$$U_K^{n+1} := u_{e,K}^{n+1} - \tilde{u}_{e,K}^{n+1}, \quad V_K^{n+1} := v_K^{n+1} - \tilde{v}_K^{n+1}, \quad W_K^{n+1} := w_K^{n+1} - \tilde{w}_K^{n+1}$$

we get

$$\frac{\beta c_{\mathrm{m}}|K|}{\Delta t}V_K^{n+1}+\sum_{\sigma\in\mathcal{E}_{\mathrm{int}}(K)}d_{\mathrm{e},\sigma}^*(U_L^{n+1}-U_K^{n+1})|K|(I_{1,\mathrm{ion}}(v_K^{n+1})-I_{1,\mathrm{ion}}(\tilde{v}_K^{n+1}))-\lambda\beta|K|W_K^{n+1}=0, \tag{3.4}$$

$$-\sum_{\sigma\in\mathcal{E}_{\mathrm{int}}(K)}(d_{\mathrm{i},\sigma}^*+d_{\mathrm{e},\sigma}^*)(U_L^{n+1}-U_K^{n+1})=\sum_{\sigma\in\mathcal{E}_{\mathrm{int}}(K)}d_{\mathrm{i},\sigma}^*(V_L^{n+1}-V_K^{n+1}), \tag{3.5}$$

$$\frac{W_K^{n+1}}{\Delta t}+bW_K^{n+1}-aV_K^{n+1}=0. \tag{3.6}$$

Next, multiplying (3.4)–(3.6) by the terms $-\Delta tU_K^{n+1}$, $\Delta t(V_K^{n+1}+U_K^{n+1})$ and ΔtW_K^{n+1}, respectively, and summing the resulting equations over $K\in\mathcal{T}$ and $n\in\{0,\dots,N-1\}$ yields

$$E_1+E_2+E_3=0, \tag{3.7}$$

where

$$\begin{aligned}
E_1:=&\sum_{n=0}^{N-1}\sum_{K\in\mathcal{T}}|K|(-\beta c_{\mathrm{m}}V_K^{n+1}U_K^{n+1}+(W_K^{n+1})^2),\\
E_2:=&\sum_{n=0}^{N-1}\Delta t\sum_{K\in\mathcal{T}}\sum_{\sigma\in\mathcal{E}_{\mathrm{int}}(K)}(d_{\mathrm{e},\sigma}^*(U_L^{n+1}-U_K^{n+1})^2\\
&+[(d_{\mathrm{i},\sigma}^*+d_{\mathrm{e},\sigma}^*)(U_L^{n+1}-U_K^{n+1})+d_{\mathrm{i},\sigma}^*(V_L^{n+1}-V_K^{n+1})][V_L^{n+1}+U_L^{n+1}-(V_K^{n+1}+U_K^{n+1})]),\\
E_3:=&\sum_{n=0}^{N-1}\Delta t\sum_{K\in\mathcal{T}}|K|(\beta(I_{1,\mathrm{ion}}(\tilde{v}_K^{n+1})-I_{1,\mathrm{ion}}(v_K^{n+1}))U_K^{n+1}+\lambda\beta W_K^{n+1}U_K^{n+1}+b(W_K^{n+1})^2-aV_K^{n+1}W_K^{n+1}).
\end{aligned}$$

Multiplying (3.4) by $\Delta t(V_K^{n+1}+U_K^{n+1})$ and summing over all $K\in\mathcal{T}$ and $n\in\{0,\dots,N-1\}$, we get

$$\begin{aligned}
&\beta c_{\mathrm{m}}\sum_{n=0}^{N-1}\sum_{K\in\mathcal{T}}|K|V_K^{n+1}(V_K^{n+1}+U_K^{n+1})+\sum_{n=0}^{N-1}\Delta t\sum_{K\in\mathcal{T}}\beta|K|(I_{1,\mathrm{ion}}(v_K^{n+1})-I_{1,\mathrm{ion}}(\tilde{v}_K^{n+1}))(V_K^{n+1}+U_{\mathrm{e},K}^{n+1})\\
&-\sum_{n=0}^{N-1}\Delta t\sum_{K\in\mathcal{T}}\lambda\beta|K|W_K^{n+1}(V_K^{n+1}+U_K^{n+1})\\
&=\sum_{n=0}^{N-1}\Delta t\sum_{K\in\mathcal{T}}\sum_{\sigma\in\mathcal{E}_{\mathrm{int}}(K)}d_{\mathrm{e},\sigma}^*(U_L^{n+1}-U_K^{n+1})[V_L^{n+1}+U_L^{n+1}-(V_K^{n+1}+U_K^{n+1})].
\end{aligned}$$

From this and (3.7), it follows that

$$\begin{aligned}
E_1+E_2+E_3\geq&\sum_{n=0}^{N-1}\sum_{K\in\mathcal{T}}|K|\{\beta c_{\mathrm{m}}(V_K^{n+1})^2+(W_K^{n+1})^2-\Delta t\lambda\beta W_K^{n+1}V_K^{n+1}\\
&+\Delta t\beta[I_{1,\mathrm{ion}}(v_K^{n+1})-I_{1,\mathrm{ion}}(\tilde{v}_K^{n+1})]V_K^{n+1}+\Delta tb(W_K^{n+1})^2-\Delta taV_K^{n+1}W_K^{n+1}\}\\
\geq&\sum_{n=0}^{N-1}\sum_{K\in\mathcal{T}}|K|\{\beta c_{\mathrm{m}}(V_K^{n+1})^2-\frac{b}{2}\Delta t(W_K^{n+1})^2-\frac{\beta^2\lambda^2}{2b}\Delta t(V_K^{n+1})^2-\beta C_I\Delta t(V_K^{n+1})^2\\
&+b\Delta t(W_K^{n+1})^2-\frac{b}{2}\Delta t(W_K^{n+1})^2-\frac{a^2}{2b}\Delta t(V_K^{n+1})^2\}.
\end{aligned}$$

Herein we have used (2.3). Consequently, combining all previous inequalities, we end up with

$$\beta c_{\mathrm{m}} \sum_{n=0}^{N-1} \sum_{K \in \mathcal{T}} |K| (V_K^{n+1})^2 \leq \left(\beta C_I + \frac{\beta^2 \lambda^2}{2b} + \frac{a^2}{2b} \right) \sum_{n=0}^{N-1} \Delta t \sum_{K \in \mathcal{T}} |K| (V_K^{n+1})^2, \tag{3.8}$$

and since

$$\sum_{K \in \mathcal{T}} |K| (V_K^{n+1})^2 > 0,$$

from (3.8) we get

$$\frac{\beta c_{\mathrm{m}}}{2\beta C_I + \frac{\beta^2 \lambda^2}{b} + \frac{a^2}{b}} \leq \frac{\beta c_{\mathrm{m}}}{\beta C_I + \frac{\beta^2 \lambda^2}{2b} + \frac{a^2}{2b}} \leq \Delta t,$$

which contradicts (2.23). □

4. A priori estimates and convergence of the scheme

First we need to establish several a priori estimates for the FV scheme, which eventually will imply the desired convergence results.

Lemma 4.1. *Let $(v_K^n, u_{\mathrm{e},K}^n, w_K^n)_{K \in \mathcal{T}, n \in \{0,\dots,N\}}$ be a solution of the FV scheme (2.15), (2.19)–(2.22). Then there exist constants $C_1, C_2, C_3 > 0$, depending on $\Omega, T, v_0, w_0, I_{\mathrm{app}}$, and α, s such that*

$$\max_{n \in \{1,\dots,N\}} \sum_{K \in \mathcal{T}} |K| ((v_K^n)^2 + (w_K^n)^2) \leq C_1, \tag{4.1}$$

$$\sum_{n=0}^{N-1} \Delta t \sum_{K \in \mathcal{T}} \sum_{\sigma = K|L \in \mathcal{E}_{\mathrm{int}}(K)} ((u_{\mathrm{e},K}^{n+1} - u_{\mathrm{e},L}^{n+1})^2 + (v_K^{n+1} + u_{\mathrm{e},K}^{n+1} - (v_L^{n+1} + u_{\mathrm{e},L}^{n+1}))^2) \leq C_2, \tag{4.2}$$

$$\sum_{n=0}^{N-1} \Delta t \sum_{K \in \mathcal{T}} |K| (|v_K^{n+1}|^4 + |I_{1,\mathrm{ion}}(v_K^{n+1})|^{4/3}) \leq C_3. \tag{4.3}$$

Proof. We multiply (2.19)–(2.21) by $-\Delta t u_{\mathrm{e},K}^{n+1}$, $\Delta t (v_K^{n+1} + u_{\mathrm{e},K}^{n+1})$ and $\Delta t w_K^{n+1}$, respectively, add the equations, sum the result over K and n, and gather by edges. This yields $F_1 + F_2 + F_3 = 0$, where

$$\begin{aligned}
F_1 :=& \sum_{n=0}^{N-1} \sum_{K \in \mathcal{T}} |K| (-\beta c_{\mathrm{m}} (v_K^{n+1} - v_K^n) u_{\mathrm{e},K}^{n+1} + (w_K^{n+1} - w_K^n) w_K^{n+1}),\\
F_2 :=& \sum_{n=0}^{N-1} \Delta t \sum_{K \in \mathcal{T}} \sum_{\sigma \in \mathcal{E}_{\mathrm{int}}(K)} (d_{\mathrm{e},\sigma}^* (u_{\mathrm{e},L}^{n+1} - u_{\mathrm{e},K}^{n+1})^2\\
&+ [(d_{\mathrm{i},\sigma}^* + d_{\mathrm{e},\sigma}^*)(u_{\mathrm{e},L}^{n+1} - u_{\mathrm{e},K}^{n+1}) + d_{\mathrm{i},\sigma}^* (v_L^{n+1} - v_K^{n+1})][v_L^{n+1} + u_{\mathrm{e},L}^{n+1} - (v_K^{n+1} + u_{\mathrm{e},K}^{n+1})]),\\
F_3 :=& \sum_{n=0}^{N-1} \Delta t \sum_{K \in \mathcal{T}} |K| (-\beta I_{\mathrm{ion},K}^{n+1} u_{\mathrm{e},K}^{n+1} + 2 I_{\mathrm{app},K}^{n+1} u_{\mathrm{e},K}^{n+1} + I_{\mathrm{app},K}^{n+1} v_K^{n+1} - H_K^{n+1} w_K^{n+1}).
\end{aligned}$$

Multiplying (2.19) by $\Delta t (v_K^{n+1} + u_{\mathrm{e},K}^{n+1})$, summing over K and n and gathering by edges leads to

$$\begin{aligned}
&\sum_{n=0}^{N-1} \Delta t \sum_{K \in \mathcal{T}} |K| (\beta c_{\mathrm{m}} (v_K^{n+1} - v_K^n)(v_K^{n+1} + u_{\mathrm{e},K}^{n+1}) + \beta I_{\mathrm{ion},K}^{n+1} (v_K^{n+1} + u_{\mathrm{e},K}^{n+1}) - I_{\mathrm{app},K}^{n+1} (v_K^{n+1} + u_{\mathrm{e},K}^{n+1}))\\
&= \sum_{n=0}^{N-1} \Delta t \sum_{K \in \mathcal{T}} \sum_{\sigma \in \mathcal{E}_{\mathrm{int}}(K)} d_{\mathrm{e},\sigma}^* (u_{\mathrm{e},L}^{n+1} - u_{\mathrm{e},K}^{n+1})[v_L^{n+1} + u_{\mathrm{e},L}^{n+1} - (v_K^{n+1} + u_{\mathrm{e},K}^{n+1})].
\end{aligned}$$

From the inequality "$a(a-b) \geq 1/2(a^2-b^2)$", and collecting and reordering the previous inequalities we obtain

$$\begin{aligned}
&\frac{\beta c_{\mathrm{m}}}{2}\sum_{K\in\mathcal{T}}|K|(v_K^N)^2+\frac{1}{2}\sum_{K\in\mathcal{T}}|K|(w_K^N)^2\\
&\leq C(c_{\mathrm{m}},C_M,C_p)\sum_{n=0}^{N-1}\Delta t\sum_{K\in\mathcal{T}}|K||I_{\mathrm{app},K}^{n+1}|^2+\sum_{K\in\mathcal{T}}|K|\left(\frac{\beta c_{\mathrm{m}}}{2}(v_K^0)^2+\frac{1}{2}(w_K^0)^2\right)\\
&\quad+(C+\beta C_I+\frac{\beta^2\lambda^2}{2b}+\frac{a^2}{2b})\sum_{n=0}^{N-1}\Delta t\sum_{K\in\mathcal{T}}|K|(v_K^{n+1})^2
\end{aligned}\tag{4.4}$$

for some constant $C>0$. Clearly, the following inequalities hold:

$$\sum_{n=0}^{N-1}\Delta t\sum_{K\in\mathcal{T}}|K||I_{\mathrm{app},K}^{n+1}|^2\leq\|I_{\mathrm{app}}\|^2_{L^2(Q_T)},\ \sum_{K\in\mathcal{T}}|K|\left(\frac{\beta c_{\mathrm{m}}}{2}(v_K^0)^2+\frac{1}{2}(w_K^0)^2\right)\leq\frac{\beta c_{\mathrm{m}}}{2}\|v_0\|^2_{L^2(\Omega)}+\frac{1}{2}\|w_0\|^2_{L^2(\Omega)}.$$

In view of (4.4), this implies the existence of constants $C_4, C_5>0$ such that

$$\sum_{K\in\mathcal{T}}|K|(v_K^N)^2\leq C_4+C_5\sum_{n=0}^{N-1}\Delta t\sum_{K\in\mathcal{T}}|K|(v_K^{n+1})^2.\tag{4.5}$$

Note that (4.5) is also true if we replace N by $n_0\in\{1,\dots,N\}$, so we have established that

$$\sum_{K\in\mathcal{T}}|K|(v_K^{n_0})^2\leq C_4+C_5\sum_{n=0}^{n_0-1}\Delta t\sum_{K\in\mathcal{T}}|K|(v_K^{n+1})^2.\tag{4.6}$$

By a discrete Gronwall inequality, we obtain from (4.6)

$$\sum_{K\in\mathcal{T}}|K|(v_K^{n_0})^2\leq C_6\tag{4.7}$$

for any $n_0\in\{1,\dots,N\}$ and some constant $C_6>0$. Then

$$\max_{n\in\{1,\dots,N\}}\sum_{K\in\mathcal{T}}|K|(v_K^n)^2\leq C_6.$$

Finally, (4.4) and (4.7) imply that there exist constants $C_7, C_8>0$ such that

$$\max_{n\in\{1,\dots,N\}}\sum_{K\in\mathcal{T}}|K|(w_K^n)^2\leq C_7,$$

$$\sum_{n=0}^{N-1}\Delta t\sum_{K\in\mathcal{T}}\sum_{\sigma=K|L\in\mathcal{E}_{\mathrm{int}}(K)}(|u_{\mathrm{e},K}^{n+1}-u_{\mathrm{e},L}^{n+1}|^2+|v_K^{n+1}+u_{\mathrm{e},K}^{n+1}-(v_L^{n+1}+u_{\mathrm{e},L}^{n+1})|^2)\leq C_8.$$

From the previous inequalities it follows that

$$0\leq\sum_{n=0}^{N-1}\Delta t\sum_{K\in\mathcal{T}}|K|I_{1,\mathrm{ion}}(v_K^{n+1})v_K^{n+1}+C_I\sum_{n=0}^{N-1}\Delta t\sum_{K\in\mathcal{T}}|K|(v_K^{n+1})^2\leq C_9$$

for some constant $C_9>0$. Using this and (4.1), we get that there exists a constant C_{10} such that

$$\sum_{n=0}^{N-1}\Delta t\sum_{K\in\mathcal{T}}|K||I_{1,\mathrm{ion}}(v_K^{n+1})v_K^{n+1}|\leq C_{10}.\tag{4.8}$$

Finally, from (2.4) and (4.8) we conclude that there exists a constant $C_{11}>0$ such that

$$\|v_h\|_{L^4(Q_T)}+\|I_{1,\mathrm{ion}}(v_h)\|_{L^{4/3}}(Q_T)\leq C_{11}.\quad\square$$

Before passing to the limit, we derive space and time translation estimates implying that the sequence v_h is relatively compact in $L^2(Q_T)$.

Lemma 4.2. *There exists a constant $C > 0$ depending on Ω, T, v_0, I_{app} and C_I such that*

$$\forall y \in \mathbb{R}^3: \quad \iint_{\Omega' \times (0,T)} |v_h(x+y,t) - v_h(x,t)|^2 \,\mathrm{d}x\,\mathrm{d}t \le C|y|(|y|+2h), \quad \Omega' := \{x \in \Omega : [x, x+y] \subset \Omega\},$$
$$\forall \tau \in (0,T): \quad \iint_{\Omega \times (0,T-\tau)} |v_h(x,t+\tau) - v_h(x,t)|^2 \,\mathrm{d}x\,\mathrm{d}t \le C\tau.$$

The proof of Lemma 4.2 is omitted since it is similar to that of Lemmas 4.3 and 4.6 in [21] (see also Lemma 6.1 in [7]).

Proof of Theorem 2.1. Due to our Lemmas 4.1 and 4.2, there exists a subsequence of $\mathbf{u}_h$, not relabeled, such that, as $h \to 0$,

$$\begin{aligned} &(i) \quad \mathbf{u}_h \to \mathbf{u} \text{ weakly in } L^2(Q_T), \\ &(ii) \quad v_h \to v \text{ strongly in } L^2(Q_T) \text{ and a.e. in } Q_T, \\ &(iii) \quad \nabla_h u_{\mathrm{e},h} \to \nabla u_{\mathrm{e}} \text{ weakly in } (L^2(Q_T))^3. \end{aligned} \tag{4.9}$$

What is left to show is that the limit functions v, u_{e}, w constructed in (4.9) actually constitute a weak solution of (1.1), (2.5), (2.6).

Let $\varphi_{\mathrm{e}}, \psi \in \mathcal{D}([0,T) \times \bar{\Omega})$ be such that the support of φ_{e} is contained in $(0,T) \times \{x \in \Omega : d(x, \partial\Omega) > h\}$ for a sufficiently small $h > 0$. Observe that $\varphi_{\mathrm{e}}(x) = 0$ if $x \in T^{\mathrm{ext}}_{K,\sigma}$, for all $\sigma \in \mathcal{E}_{\mathrm{ext}}(K)$ and $K \in \mathcal{T}$. We multiply (2.19) by $\Delta t \varphi_{\mathrm{e}}(x_K, t^n)$. Summing the result over K and n gives $\beta c_{\mathrm{m}} G_1 + G_2 + \beta G_3 + \beta G_4 = G_5$, where we define

$$\begin{aligned} G_1 &:= \sum_{n=0}^{N-1} \sum_{K \in \mathcal{T}} |K| (v_K^{n+1} - v_K^n) \varphi_{\mathrm{e}}(x_K, t^n), \\ G_2 &:= \sum_{n=0}^{N-1} \Delta t \sum_{K \in \mathcal{T}} \sum_{\sigma \in \mathcal{E}_{\mathrm{int}}(K)} d^*_{\mathrm{e},\sigma} (u^{n+1}_{\mathrm{e},L} - u^{n+1}_{\mathrm{e},K}) \varphi_{\mathrm{e}}(x_K, t^n), \\ G_3 &:= \sum_{n=0}^{N-1} \Delta t \sum_{K \in \mathcal{T}} |K| I_{1,\mathrm{ion}}(v_K^{n+1}) \varphi_{\mathrm{e}}(x_K, t^n), \quad G_4 := -\lambda \sum_{n=0}^{N-1} \Delta t \sum_{K \in \mathcal{T}} |K| w_K^{n+1} \varphi_{\mathrm{e}}(x_K, t^n), \\ G_5 &:= \sum_{n=0}^{N-1} \Delta t \sum_{K \in \mathcal{T}} |K| I^{n+1}_{\mathrm{app},K} \varphi_{\mathrm{e}}(x_K, t^n). \end{aligned} \tag{4.10}$$

Performing integration by parts and keeping in mind that $\varphi_{\mathrm{e}}(T, x_K) = 0$ for all $K \in \mathcal{T}$, we obtain

$$\begin{aligned} G_1 &= -\sum_{n=0}^{N-1} \sum_{K \in \mathcal{T}} |K| v_K^{n+1} (\varphi_{\mathrm{e}}(x_K, t^{n+1}) - \varphi_{\mathrm{e}}(x_K, t^n)) - \sum_{K \in \mathcal{T}} |K| v_K^0 \varphi_{\mathrm{e}}(x_K, 0) \\ &= -\sum_{n=0}^{N-1} \sum_{K \in \mathcal{T}} \int_{t^n}^{t^{n+1}} \int_K v_K^{n+1} \partial_t \varphi_{\mathrm{e}}(x_K, t) \,\mathrm{d}x\,\mathrm{d}t - \sum_{K \in \mathcal{T}} \int_K v_0(x) \varphi_{\mathrm{e}}(0, x_K) \,\mathrm{d}x =: -G_{1,1} - G_{1,2}. \end{aligned}$$

Let us also introduce

$$G^*_1 = -\sum_{n=0}^{N-1} \sum_{K \in \mathcal{T}} \int_{t^n}^{t^{n+1}} \int_K v_K^{n+1} \partial_t \varphi_{\mathrm{e}}(x, t) \,\mathrm{d}x\,\mathrm{d}t - \int_\Omega v_0(x) \varphi_{\mathrm{e}}(x, 0) \,\mathrm{d}x =: -G^*_{1,1} - G^*_{1,2}.$$

Then

$$G_{1,2} - G^*_{1,2} = \sum_{K \in \mathcal{T}} \int_K v_0(x) (\varphi_{\mathrm{e}}(x_K, 0) - \varphi_{\mathrm{e}}(x, 0)) \,\mathrm{d}x.$$

By the regularity of φ_e, there exists a constant $C > 0$ such that

$$|\varphi_e(x_K, 0) - \varphi_e(x, 0)| \leq Ch.$$

This implies

$$|G_{1,2} - G^*_{1,2}| \leq Ch \sum_{K \in \mathcal{T}} \int_K |v_0(x)| \, dx. \tag{4.11}$$

Sending $h \to 0$ in (4.11) we arrive at

$$\lim_{h \to 0} |G_{1,2} - G^*_{1,2}| = 0.$$

Next, note that

$$G_{1,1} - G^*_{1,1} = \sum_{n=0}^{N-1} \sum_{K \in \mathcal{T}} v_K^{n+1} \int_{t^n}^{t^{n+1}} \int_K (\partial_t \varphi_e(x_K, t) - \partial_t \varphi_e(x, t)) \, dx \, dt,$$

and hence from the regularity of $\partial_t \varphi_e$ and Hölder's inequality, we obtain

$$|G_{1,1} - G^*_{1,1}| \leq C(h) \left(\sum_{n=0}^{N-1} \Delta t \sum_{K \in \mathcal{T}} |K| (v_K^{n+1})^2 \right)^{1/2},$$

where $C(h) > 0$ is a function satisfying $C(h) \to 0$ as $h \to 0$. In view of (4.1), we conclude that

$$\lim_{h \to 0} |G_{1,1} - G^*_{1,1}| = 0.$$

Handling the other terms in (4.10) similarly (see [7] for details) yields

$$\lim_{h \to 0} G_2 = \int_0^T \int_\Omega \mathbf{M}_e(x) \nabla u_e \cdot \nabla \varphi_e \, dx \, dt, \quad \lim_{h \to 0} G_4 = -\lambda \beta \int_0^T \int_\Omega w \varphi_e \, dx \, dt,$$
$$\lim_{h \to 0} G_3 = \int_0^T \int_\Omega I_{1,\text{ion}}(v) \varphi_e \, dx \, dt, \qquad \lim_{h \to 0} G_5 = \int_0^T \int_\Omega I_{\text{app}} \varphi_e \, dx \, dt,$$

which yields that the Eq. (2.9) hold. This concludes the proof of Theorem 2.1. □

5. Numerical examples

5.1. Example 1 (2D reduced monodomain model)

First, as a test case, we consider a simplification of the monodomain problem (1.2) consisting in taking only the first equation of (1.2). In such case, the gating variable does not exist, and $I_{\text{app}} = 0$. Moreover, Dirichlet boundary conditions are imposed on the left and right boundaries of the domain $\bar{\Omega} = [0, 1\,\text{cm}]^2$ ($v(0, y, t) = 1$ and $v(1, y, t) = 1$) while homogeneous conditions are imposed on the rest of the boundary. The function I_{ion} in (1.2) correspond to the FitzHugh-Nagumo model (2.1), where the parameters involved are chosen such that the problem possesses the following analytical solution

$$v(x, y, t) = \left\{ 1 + 0.0001 \exp\left(\sqrt{\frac{1}{2}} (x - C_0 t) \right) \right\}^{-1},$$

as proposed in [4]. This is, $\beta = 1$, $c_m = 1$, $(1 + \mu)^{-1} \mathbf{M}_i = C_1$, $C_0 = \sqrt{-\lambda C_1/2}(-2\alpha + 1)$, $C_1 = 1.6$, $\lambda = -1.6$ and $\theta = 0.25$. The initial solution is then given by $v_0(x, y) = v(x, y, 0)$.

Even though the gating variable is absent, the reduced model provides a known exact solution and it serves as a prototype to validate the numerical method. Of course, the corresponding FV scheme needs to be properly adjusted to handle Dirichlet boundary conditions. The convergence analysis in that case is covered by the result presented in [7].

Table 1
Example 1 (reduced monodomain model): number of control volumes $\mathcal{N}$, meshsize h, approximate L^1–errors for v and observed convergence rates r^1 at simulated time t.

$\mathcal{N}$	h	Time, $t = 10$ ms		Time, $t = 25$ ms		Time, $t = 50$ ms	
		L^1–error	r^1	L^1–error	r^1	L^1–error	r^1
1024	0.0312	2.31×10^{-3}	–	3.11×10^{-3}	–	6.37×10^{-4}	–
4096	0.0156	1.27×10^{-3}	1.2766	7.21×10^{-4}	1.2509	3.19×10^{-4}	1.2694
16,384	0.0078	7.81×10^{-4}	1.2514	3.05×10^{-4}	1.2478	9.46×10^{-5}	1.2761
65,536	0.0039	4.02×10^{-4}	1.2401	1.47×10^{-4}	1.2426	5.10×10^{-5}	1.2518

Table 1 provides the error history for the reduced monodomain model when compared with the analytical solution. An approximate order of convergence around $h^{1.25}$ is obtained. By rate of convergence for the scalar field z, we mean

$$r(z) = \frac{\log(e(z)/e^*(z))}{\log(h/h^*)},$$

where $e(z)$ and $e^*(z)$ denote the respective errors computed for two consecutive meshes of sizes h and h^*.

5.2. Example 2 (3D monodomain model)

Now we solve numerically the simple monodomain model (1.2) with homogeneous Neumann boundary conditions. The ionic current and membrane model are determined by the FitzHugh-Nagumo membrane kinetics (2.1), with the following parameters (see [5]): $a = 0.16875$, $b = 1.0$, $\lambda = -100$ and $\theta = 0.25$. The computational domain is the cube $\bar{\Omega} = [0, 1\,\text{cm}]^3$, the number of control volumes is $\mathcal{N} = 262,144$ and the remaining parameters are $c_m = 1.0\,\text{mF/cm}^2$ and $\beta = 1.0\,\text{cm}^{-1}$. The unit for v and w is mV. We consider in (1.2)$(1+\mu)^{-1}\mathbf{M}_i$:=diag(γ, γ, γ) with $\gamma = 0.01$, and the respective initial data for v and w are given by

$$v_0(x, y, z) = \left(1 - \frac{1}{1 + \exp(-50(x^2 + y^2 + z^2)^{1/2} - 0.1)}\right) \text{mV}, \quad w_0 = 0\,\text{mV}.$$

The electrical activity in the cubic domain during a period of 45 ms is illustrated in Fig. 1. Here, snapshots of the corresponding numerical solution at different times are shown. We only display the potential field, which behaves as a travelling front going symmetrically from the origin towards the corner (1 cm, 1 cm, 1 cm). The parameters have been chosen so that the travelling waves produced have positive speed, but less than one.

For our simulations of Examples 2 and 3, for which exact solutions are not available, we compute errors in different norms using a numerical solution on a fine mesh (of 5,832,000 and 1,048,576 grid points for Examples 2 and 3 , respectively) as a reference solution. Then, to measure errors between a reference solution z_{ref} and an approximate

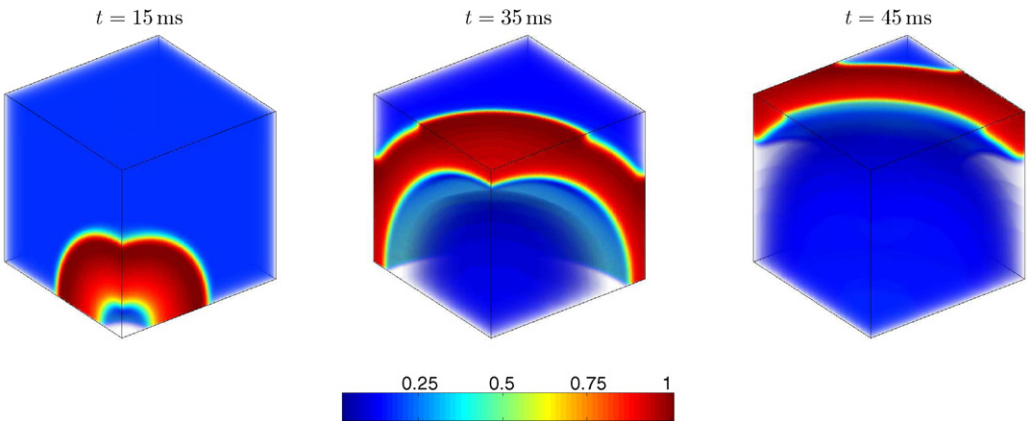

Fig. 1. Example 2 (monodomain model): numerical solution v [mV] at different times.

Table 2
Example 2 (monodomain model): number of control volumes $\mathcal{N}$, meshsize h, approximate L^1–errors for v and observed convergence rates r^1 at simulated time t.

$\mathcal{N}$	h	Time, $t = 15$ ms		Time, $t = 35$ ms		Time, $t = 45$ ms	
		L^1–error	r^1	L^1–error	r^1	L^1–error	r^1
4096	0.0625	5.68×10^{-2}	–	2.34×10^{-2}	–	9.12×10^{-3}	–
32,768	0.0313	2.58×10^{-2}	1.2412	1.07×10^{-2}	1.2315	4.26×10^{-3}	1.1982
262,144	0.0156	1.22×10^{-2}	1.2356	4.91×10^{-3}	1.2238	1.89×10^{-3}	1.2725
2,097,152	0.0078	5.71×10^{-3}	1.1936	2.28×10^{-3}	1.2067	8.91×10^{-4}	1.1849

solution z_h, we will use L^p-errors: $e_p = \|z^n_{\text{ref}} - z^n_h\|_p$, $p = 1, 2, \infty$, where

$$e_\infty = \max_{K \in \mathcal{T}} |z^n_{\text{ref},K} - z^n_{hK}|; \quad e_p = \left(\frac{1}{|K|} \sum_{K \in \mathcal{T}} |z^n_{\text{ref},K} - z^n_{hK}|^p \right)^{1/p}, \quad p = 1, 2.$$

Here $z^n_{r,K}$ stands for the projection of the reference solution onto the control volume K.

For Example 2 the corresponding convergence history is given in Table 2. From this information we point out that the method provides a rate of convergence around $h^{1.2}$.

5.3. Example 3 (2D bidomain model)

As a third example, consider a two-dimensional slab $\bar{\Omega} = [0, 1\,\text{cm}]^2$, and the bidomain model (1.1). In light of Remark 2.1 it is clear that the FV scheme introduced does not apply to the fully anisotropic case due to the non-consistency of the flux computations. Therefore we assume that the fibers are aligned with the axes and consider the parameters (see [5]) $c_m = 1.0\,\text{mF/cm}^2$, $\sigma_i^l = 3.0 \times 10^{-3}\,\Omega^{-1}\,\text{cm}^{-1}$, $\sigma_i^t = 3.1525 \times 10^{-4}\,\Omega^{-1}\,\text{cm}^{-1}$ $\sigma_e^l = 2.0 \times 10^{-3}\,\Omega^{-1}\,\text{cm}^{-1}$, $\sigma_e^t = 1.3514 \times 10^{-3}\,\Omega^{-1}\,\text{cm}^{-1}$, $\beta = 100\,\text{cm}^{-1}$, $R_m = 2.5 \times 10^3\,\Omega\,\text{cm}^2$, $v_p = 100\,\text{mV}$, $\eta_1 = 0.0044$, $\eta_2 = 0.12$, $\eta_3 = 1$, $\eta_4 = 13$ and $\eta_5 = 0.15$. The initial data is given by an initial stimulus of 1 mV applied to the center of the extracellular medium and smooth initial distributions for the transmembrane potential and gating variable.

The simulation is performed on regular mesh of $\mathcal{N} = 65,536$ control volumes with which we obtain the numerical solutions for the extracellular and transmembrane potentials shown in Fig. 2. Due to the lack of exact solutions for these examples, we compute errors in different norms using a numerical solution on a extremely fine mesh (of 1,048,576 control volumes) as reference. In addition, from Tables 3 and 4 it is observed that the rates of convergence provided by the method are slightly higher than $\mathcal{O}(h)$ for both components of the solution, but still lower than the rates obtained for the monodomain case. This behavior of the experimental rates of convergence can be also observed from Fig. 3, where we show the meshsize and errors in different norms plotted in a log-log fashion against the number of control volumes.

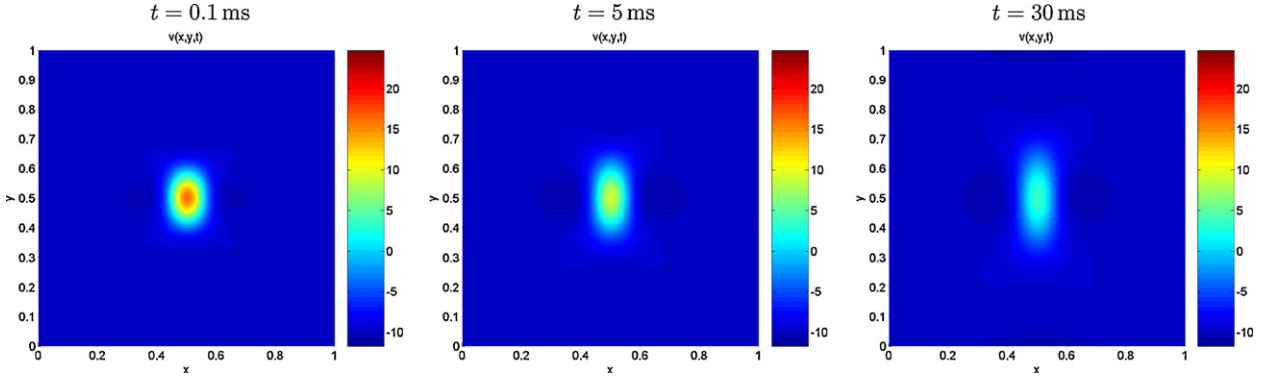

Fig. 2. Example 3 (bidomain model): transmembrane potential v [mV] at different times.

Table 3
Example 3 (bidomain model): number of control volumes $\mathcal{N}$, meshsize h, approximate errors for v in different norms and observed convergence rates r^1, r^2 and r^∞ at simulated time t.

Time	$\mathcal{N}$	L^1–error	$r^1(v)$	L^2–error	$r^2(v)$	L^∞–error	$r^\infty(v)$
$t = 0.1$ ms	1024	6.13×10^{-3}	–	4.79×10^{-3}	–	6.50×10^{-3}	–
	4096	3.07×10^{-3}	1.0124	2.31×10^{-3}	1.0253	3.17×10^{-3}	1.0378
	16,384	1.12×10^{-3}	1.0889	9.85×10^{-4}	1.0831	1.26×10^{-3}	1.0803
	65,536	5.87×10^{-4}	1.0847	4.69×10^{-4}	1.0982	6.07×10^{-4}	1.0894
$t = 5$ ms	1024	3.21×10^{-3}	–	3.01×10^{-4}	–	7.14×10^{-3}	–
	4096	1.30×10^{-3}	1.0153	1.21×10^{-4}	0.9831	3.54×10^{-3}	1.0933
	16,384	5.74×10^{-4}	1.0893	5.72×10^{-5}	1.1123	5.23×10^{-4}	1.0937
	65,536	2.72×10^{-4}	1.1018	2.43×10^{-5}	1.0284	2.88×10^{-4}	1.0874
$t = 35$ ms	1024	1.64×10^{-3}	–	2.92×10^{-3}	–	1.05×10^{-2}	–
	4096	7.39×10^{-4}	1.0983	1.40×10^{-3}	0.9821	4.67×10^{-3}	0.9732
	16,384	3.28×10^{-4}	1.0972	6.82×10^{-4}	1.0024	2.13×10^{-3}	1.0536
	65,536	1.57×10^{-4}	1.0866	2.97×10^{-4}	1.1321	9.72×10^{-4}	1.0952

Table 4
Example 3 (bidomain model): number of control volumes $\mathcal{N}$, meshsize h, approximate errors for u_e in different norms and observed convergence rates r^1, r^2 and r^∞ at simulated time t.

Time	$\mathcal{N}$	L^1–error	$r^1(u_e)$	L^2–error	$r^2(u_e)$	L^∞–error	$r^\infty(u_e)$
$t = 0.1$ ms	1024	2.31×10^{-4}	–	2.46×10^{-4}	–	3.52×10^{-4}	–
	4096	3.77×10^{-5}	1.0815	4.06×10^{-5}	1.1073	6.26×10^{-5}	1.0332
	16,384	6.19×10^{-6}	1.0950	6.80×10^{-6}	1.0952	1.06×10^{-5}	1.0849
	65,536	1.21×10^{-6}	1.0781	1.09×10^{-6}	1.1031	1.72×10^{-6}	1.1216
$t = 5$ ms	1024	4.53×10^{-4}	–	4.47×10^{-4}	–	6.36×10^{-4}	–
	4096	7.28×10^{-5}	1.1357	1.06×10^{-4}	1.0678	1.04×10^{-4}	1.1131
	16,384	1.17×10^{-5}	1.0934	2.82×10^{-5}	1.1096	1.77×10^{-5}	1.0937
	65,536	2.94×10^{-6}	1.0980	4.13×10^{-6}	1.0865	2.64×10^{-6}	1.0534
$t = 35$ ms	1024	8.46×10^{-4}	–	1.02×10^{-3}	–	9.83×10^{-4}	–
	4096	1.36×10^{-4}	1.1277	1.69×10^{-4}	1.0662	1.98×10^{-4}	1.0750
	16,384	2.26×10^{-5}	1.1064	2.94×10^{-5}	1.1018	3.83×10^{-5}	1.0754
	65,536	3.73×10^{-6}	1.1080	5.91×10^{-6}	1.0962	6.29×10^{-6}	1.0804

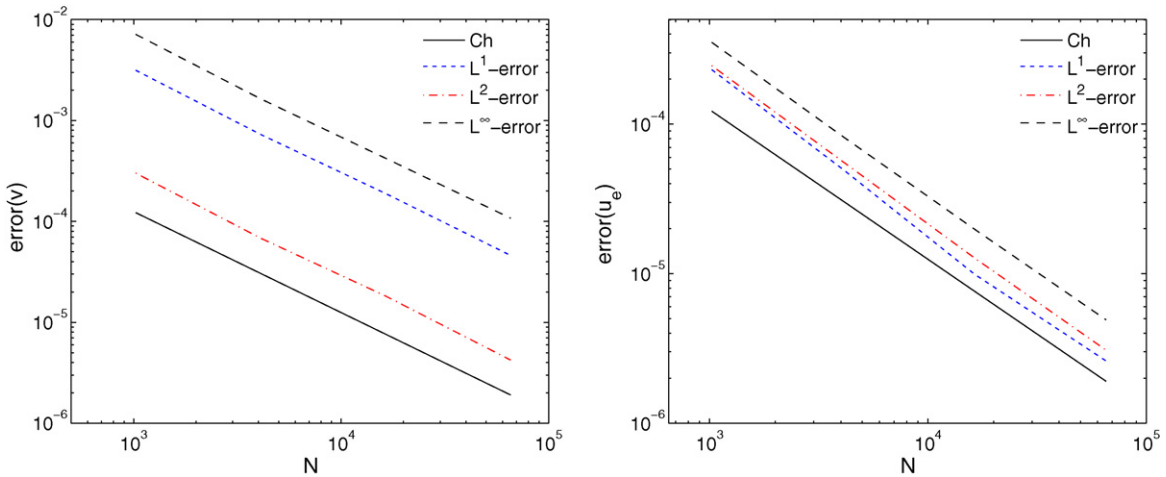

Fig. 3. Example 3 (bidomain model): meshsize h and errors for v (left) and u_e (right) in different norms versus the number of control volumes $\mathcal{N}$. The simulated time is $t = 5$ ms.

6. Conclusion

In this paper we have presented an implicit FV scheme for solving the bidomain model for simulating the propagation of action potential in the cardiac tissue. We emphasize that the main contribution of this work is a rigorous convergence analysis for a FV scheme, which addresses, however, only a strongly simplified version (especially, in terms of geometry of the tissue patch and complexity of the membrane model) of scenarios that are of practical interest in electrocardiology. In particular, the isotropy assumption, required for the convergence proof, is removed in work in progress (see [2]).

Concerning the membrane kinetics, we are aware that the simple FitzHugh-Nagumo model (2.1) has reduced significance for real-world cardiac simulations, and that more complex cell models such as the BRDR model [3,20,31], Luo-Rudy I [14,25] or Luo-Rudy II [26,27] (see [23] for an overview) represent the state of the art. These models consider large numbers (up to 15, in the case of Luo-Rudy II) of ionic currents, and a corresponding number of gating variables. These gating variables give rise to additional ordinary differential equations, while the present model includes just one scalar equation, namely (1.1c). Of course, from the computational viewpoint, apart from the complexity of solving a larger ODE system in each time step, there is no basic difficulty associated with the numerical solution of these equations, especially since the spatial coherence is always achieved via the diffusion of the electric potentials u_e and v, as in our model. In other words, considering a more complex cell model does not affect the number and structure of the PDEs of the bidomain model. However, the present paper addresses the more fundamental issue of well-posedness and convergence of a finite volume scheme, and the proofs of Lemmas 3.3 and 4.1, for example, which in turn are standard steps in the analysis of a FV scheme, strongly depend on the particular algebraic form of the FitzHugh-Nagumo membrane model (2.1). (Restrictions of the algebraic form of I_{ion} were also imposed in the convergence analysis by Bendahmane and Karlsen [7].) Consequently, even though the present FV scheme can possibly be combined with more complex membrane models, an open issue is whether the convergence analysis can be extended to such cases.

As in many applications, experience of scientific computing is here much ahead of the results of rigorous convergence analysis. In fact, an exploratory study with an adaptive multiresolution implementation similar to [5,10] for the bidomain model with Luo-Rudy II kinetics is under preparation.

The approach of the present paper, which is based on the main assumption of isotropic conductivities for both media, enables us to use classical tools in the study of the FV scheme. A rigorous analysis, which conforms the main result of the present work, shows that the proposed numerical method converges to the corresponding weak solution of the problem. Moreover, preliminary numerical results carried out on simplified 2D and 3D geometries confirm the good qualitative behaviour of our approach, while experimental rates of convergence of order h are obtained. Finally, we mention that the CPU effort needed for solving the PDE system in each time step is proportional to $\mathcal{N}$, this part of the method is therefore dominant in the overall algorithm, which for the computation until a finite time, using a structured mesh, has complexity of $\mathcal{O}(h^{-4})$. This complexity is drastically reduced when using an adaptive strategy such as a multiresolution scheme [5].

Acknowledgments

MB acknowledges support by Fondecyt project 1070682, RB acknowledges partial support by Fondecyt project 1090456, Fondap in Applied Mathematics, project 15000001, and BASAL project CMM, Universidad de Chile and by Centro de Investigación en Ingeniería Matemática (CI^{2}MA), Universidad de Concepción. The work of RR is supported by the European Research Council Advanced Grant "Mathcard, Mathematical Modelling and Simulation of the Cardiovascular System", Project ERC-2008-AdG 227058.

References

[1] B. Andreianov, M. Bendahmane, K.H. Karlsen, Finite volume schemes for doubly nonlinear degenerate parabolic equations, J. Hyp. Diff. Eqn., in press.
[2] B. Andreianov, M. Bendahmane, K.H. Karlsen, C. Pierre, Convergence of discrete duality finite volume schemes for the macroscopic bidomain model of the heart electric activity, in preparation.
[3] G.W. Beeler, H. Reuter, Reconstruction of the action potential of ventricular myocardial fibres, J. Physiol. 268 (1977) 177–210.
[4] Y. Belhamadia, A time dependent adaptive remeshing for electrical waves of the heart, IEEE Trans. Biomed. Eng. 55 (2007) 443–452.

[5] M. Bendahmane, R. Bürger, R. Ruiz-Baier, A multiresolution space–time adaptive scheme for the bidomain model in electrocardiology, Numer. Meth. Partial Diff. Eqn., in press.
[6] M. Bendahmane, K.H. Karlsen, Analysis of a class of degenerate reaction–diffusion systems and the bidomain model of cardiac tissue, Netw. Heterog. Media 1 (2006) 185–218.
[7] M. Bendahmane, K.H. Karlsen, Convergence of a finite volume scheme for the bidomain model of cardiac tissue, Appl. Numer. Math. 59 (2009) 2266–2284.
[8] M.J. Berger, J. Oliger, Adaptive mesh refinement for hyperbolic partial differential equations, J. Comput. Phys. 53 (1984) 482–512.
[9] Y. Bourgault, Y. Coudière, C. Pierre, Existence and uniqueness of the solution for the bidomain model used in cardiac electro-physiology, Nonlin. Anal. Real World Appl. 10 (2009) 458–482.
[10] R. Bürger, R. Ruiz-Baier, K. Schneider, Adaptive multiresolution methods for the simulation of waves in excitable media. Preprint 2009–11, Departamento de Ingeniería Matemática, Universidad de Concepción, submitted for publication.
[11] E. Cherry, H. Greenside, C.S. Henriquez, Efficient simulation of three-dimensional anisotropic cardiac tissue using an adaptive mesh refinement method, Chaos 13 (2003) 853–865.
[12] P. Colli Franzone, P. Deuflhard, B. Erdmann, J. Lang, L.F. Pavarino, Adaptivity in space and time for reaction–diffusion systems in electrocardiology, SIAM J. Sci. Comput. 28 (2006) 942–962.
[13] P. Colli Franzone, L.F. Pavarino, A parallel solver for reaction–diffusion systems in computational electro-cardiology, Math. Models Meth. Appl. Sci. 14 (2004) 883–911.
[14] P. Colli Franzone, L.F. Pavarino, B. Taccardi, Simulating patterns of excitation, repolarization and action potential duration with cardiac bidomain and monodomain models, Math. Biosci. 197 (2005) 35–66.
[15] P. Colli Franzone, L.F. Pavarino, B. Taccardi, Monodomain simulations of excitation and recovery in cardiac blocks with intramural heterogeneity, in: A. Frangi, et al. (Eds.), Functional Imaging and Modeling of the Heart (FIMH05), Springer LNCS, vol. 3504, 2005, pp. 267–277.
[16] P. Colli Franzone, G. Savaré, Degenerate evolution systems modeling the cardiac electric field at micro- and macroscopic level, in: A. Lorenzi, B. Ruf (Eds.), Evolution Equations, Semigroups and Functional Analysis, Birkhäuser, Basel, 2002, pp. 49–78.
[17] Y. Coudière, Th. Gallouët, R. Herbin, Discrete Sobolev inequalities and L^p error estimates for finite volume solutions of convection diffusion equations, M2AN Math. Model. Numer. Anal. 35 (2001) 767–778.
[18] Y. Coudière, C. Pierre, Stability and convergence of a finite volume method for two systems of reaction–diffusion in electro-cardiology, Nonlin. Anal. Real World Appl. 7 (2006) 916–935.
[19] Y. Coudière, C. Pierre, R. Turpault, Solving the fully coupled heart and torso problems of electro cardiology with a 3D discrete duality finite volume method, HAL preprint (2006). Available from http://hal.archives-ouvertes.fr/ccsd-00016825.
[20] J.P. Drouhard, F.A. Roberge, Revised formulation of the Hodgkin–Huxley representation of the sodium current in cardiac cells, Comput. Biomed. Res. (1987) 333–350.
[21] R. Eymard, Th. Gallouët, R. Herbin, Finite volume methods, in: P.G. Ciarlet, J.-L. Lions (Eds.), in: Handbook of Numerical Analysis, vol. VII, North-Holland, Amsterdam, 2000, pp. 713–1020.
[22] D. Harrild, C.S. Henriquez, A finite volume model of cardiac propagation, Ann. Biomed. Eng. 25 (1997) 315–334.
[23] J. Keener, J. Sneyd, Mathematical Physiology, second ed., vol. I–II, Springer, New York, 2009.
[24] J.-L. Lions, Quelques Méthodes de Résolution Des Problèmes Aux Limites Non Linéaires, Dunod, Paris, 1969.
[25] C.H. Luo, Y. Rudy, A model of the ventricular action potential, Circ. Res. 68 (1991) 1501–1526.
[26] C.H. Luo, Y. Rudy, A dynamic model of the cardiac ventricular action potential. I. Simulations of ionic currents and concentration changes, Circ. Res. 74 (1994) 1071–1096.
[27] C.H. Luo, Y. Rudy, A dynamic model of the cardiac ventricular action potential. II. After depolarilzations, triggered activity, and potentiation, Circ. Res. 74 (1994) 1097–1113.
[28] C. Mitchell, D. Schaeffer, A two-current model for the dynamic of cardiac membrane, Bull. Math. Biol. 65 (2001) 767–793.
[29] W. Quan, S. Evans, H. Hastings, Efficient integration of a realistic two-dimensional cardiac tissue model by domain decomposition, IEEE Trans. Biomed. Eng. 45 (1998) 372–385.
[30] H. Saleheen, K. Ng, A new three-dimensional finite-difference bidomain formulation for inhomogeneous anisotropic cardiac tissues, IEEE Trans. Biomed. Eng. 45 (1998) 15–25.
[31] K. Skouibine, N. Trayanova, P. Moore, A numerically efficient model for simulation of defibrillation in an active bidomain sheet of myocardium, Math. Biosci. 166 (2000) 85–100.
[32] J. Sundnes, G.T. Lines, X. Cai, B.F. Nielsen, K.-A. Mardal, A. Tveito, Computing the Electrical Activity in the Heart, Springer-Verlag, Berlin, 2006.
[33] J. Sundnes, G.T. Lines, A. Tveito, An operator splitting method for solving the bidomain equations coupled to a volume conductor model for the torso, Math. Biosci. 194 (2005) 233–248.
[34] M. Trew, I. Grice, B. Smaill, A. Pullan, A finite volume method for modeling discontinuous electrical activation in cardiac tissue, Ann. Biomed. Eng. 33 (2005) 590–602.
[35] M. Veneroni, Reaction–diffusion systems for the macroscopic bidomain model of the cardiac electric field, Nonlin. Anal. Real World Appl. 10 (2009) 849–868.